In Algorithms for Synthetic Aperture Radar XII, (Proc. SPIE 5808), SPIE Defense and Security Symposium, March 28 - April 1, 2005.

Three-dimensional Target Visualization from Wide-angle IFSAR Data

Randolph L. Moses[a], Paul Adams[b], and Tom Biddlecome[b]

[a]The Ohio State University, Department of Electrical and Computer Engineering
2015 Neil Avenue, Columbus, OH 43210, USA (moses.2@osu.edu)
[b]U.S. Army Research and Development Center, Vicksburg, MS
(Paul.Adams@erdc.usace.army.mil; Tommy.L.Biddlecome@erdc.usace.army.mil)

ABSTRACT

We consider the problem of developing three-dimensional (3D) spatial representations of objects by processing sparse, wide-angle radar measurements of that object. We propose an approach in which multiple interferometric SAR (IFSAR) image pairs are obtained, each using a modest angular aperture. Each IFSAR image pair is used to extract 3D scattering locations and attributes, and these points are noncoherently combined to form object reconstructions. Volume rendering methods are employed to represent these spatial points and their attributes. Reconstruction results are presented using synthetically-generated, wide-angle scattering data of a backhoe.

Keywords: synthetic aperture radar, three-dimensional reconstruction, visualization

1. INTRODUCTION

We consider the problem of developing three-dimensional (3D) spatial representations of objects by processing radar measurements of that object. In particular, we are interested in measurements that are wideband and that are collected across wide angular apertures in both azimuth and elevation. The goal is to provide 3D spatial reconstructions that can be used (a) for visualization of the object and its associated radar scattering features (such as polarization features), and (b) for automatic target recognition applications. Thus, visualization provides a mechanism for human-aided target recognition and also serves as a qualitative means for assessing the utility of extracted feature sets for automatic target recognition.

Traditional approaches for 3D synthetic aperture radar processing form a 3D spatial reconstruction from a dense set of measurements over a frequency-azimuth-elevation data cube. While such an approach has several merits, it also has some disadvantages. First, the measurement and processing requirements are significant. For example, a 3D SAR image with spatial resolution of 0.15 m requires collection of phase-coherent data over approximately 1.2 GHz in frequency and over a $6^\circ \times 6^\circ$ azimuth-elevation sector. In addition, coherent processing of this data cube imposes significant memory and computational demands. Finally, traditional SAR imaging techniques implicitly assume that scattering responses persist across the measurement aperture, an assumption that becomes tenuous for wide aperture measurements. So, even if one can overcome the significant challenges of data collection, storage, and processing of filled wide-angle apertures, traditional tomographic processing of data deserves reconsideration in light of this scattering persistence assumption.

We consider an alternative approach for forming 3D reconstructions, one that uses a sparse set of measurements over wide angles. In the proposed approach, measurements are collected as a set of high-resolution interferometric SAR (IFSAR) image pairs that are distributed over wide angles. Each image pair is coherently processed to estimate 3D scattering center locations, and associated scattering attributes, over a limited aperture. These attributed points are combined *noncoherently* to form the 3D reconstructions. The noncoherent combination is significant because it relaxes the requirement for phase coherence across wide angle apertures; in particular, multiple radar measurement platforms operating incoherently from one another are able to collect data for this reconstruction.

The proposed IFSAR processing procedure results in a set of 3D spatial point locations of scattering centers attributed by a vector of real-valued features. Analysis and visualization of this high-dimensional data represents a second challenge. We present volume rendering results in which volume clouds with varying colors and transparencies are used to represent the data.

We illustrate the processing and visualization approach using synthetic, wide-angle scattering data of a backhoe. Results are presented in which scattering amplitude, polarization parameters, and observation angle parameters are represented in the reconstructions. The reconstructions indicate the power of the proposed visualization techniques for understanding high-dimensional point data.

2. WIDE-ANGLE RADAR SCATTERING

Our goal is to develop 3D reconstructions of objects from monostatic, far-field radar backscatter measurements that may possibly span a wide range of frequencies, azimuths, and elevations, and may possibly contain multiple polarizations. These backscatter measurements can be written as

$$S(f,\phi,\psi) = \begin{bmatrix} S_{HH}(f,\phi,\psi) & S_{HV}(f,\phi,\psi) \\ S_{VH}(f,\phi,\psi) & S_{VV}(f,\phi,\psi) \end{bmatrix} \tag{1}$$

where f is the measurement frequency, and where (ϕ,ψ) denote the azimuth and elevation angle (with respect to the object) that the measurement is taken. The subscripts in equation (1) denote the receive and transmit polarization of the measurement.

Reconstruction is the process of transforming backscattering measurements into a three-dimensional (3D) spatial representation of the object. Typical reconstruction methods include synthetic aperture radar (SAR) image formation, in which a set of 2D measurements in a frequency-angle interval (e.g. $[f_L, f_H] \times [\phi_L, \phi_H]$ for a fixed ψ) is used to form an image that represents radar backscatter as a function of two spatial dimensions in an image plane. 3D SAR is a generalization in which the data is a "cube" in (f,ϕ,ψ)-space, and a 3D spatial backscattering representation is obtained. Both methods typically employ tomographic processing, and thus implicitly assume that the scattering response at spatial location (x,y,z) is constant over the (f,ϕ) or (f,ϕ,ψ) measurement interval. This constant-response assumption is reasonable for narrow percent bandwidth frequency intervals and narrow angular intervals. However, over wide percent bandwidth measurements and over wide interrogation angle widths, scattering can exhibit significant variation.[1] For such cases, traditional SAR image or volume reconstruction methods are not well-matched to this problem.[2,3]

In general, the backscattered response at location (x,y,z) on the object depends on frequency, angle, and polarization; this response can be thought of as an "antenna pattern" whose amplitude and phase depend on both angle (azimuth and elevation) and polarization. Thus, each location in the reconstruction volume is characterized by a set of features describing the polarimetric response as a function of angles ϕ and ψ. In addition, the angle-dependent and polarization-dependent properties of scattering are strongly related to the local shape of the scattering object; in particular, curvature, and orientation determine the scattering behavior.[1] As a result, 3D reconstructions that incorporate and represent these features can provide strong indications to object shape.

A complete 3D reconstruction requires coherently measuring the object over all frequencies and angles; this results in a measurement "data dome" in frequency-aspect space (or k-space) shown in Figure 1. This represents an enormous amount of data and poses significant challenges in both the acquisition and the processing of the data. Thus, 3D reconstruction methods based on sparse subsets of the data dome are of interest.

3. SPARSE APERTURE 3D RECONSTRUCTION

We consider a sparse reconstruction technique in which both the data collection and data processing requirements are simplified by exploiting properties of radar scattering physics. These properties are discussed below.

Limited Persistence of Scattering: Since object scattering behavior over wide angles is not well-modeled as independent of angle, small-angle scattering assumptions that form the basis of most current object reconstruction methods are not valid. Most scattered energy from objects of interest have limited angles of persistence, and motivates developing reconstruction algorithms that accommodate limited persistence.

In particular, limited persistence suggests a *noncoherent* combination of information from subapertures of wide-angle measurements.[2,3] We extract scattering information from limited-angle SAR images, where the angle

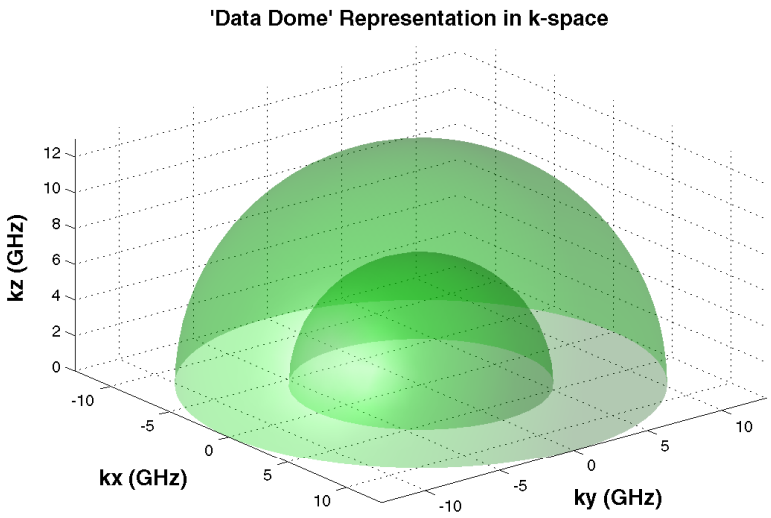

Figure 1. An X-band data dome of frequency-angle measurements for complete object reconstruction.

extent of the data used to form the image is matched to the persistence angle of scattering. We adopt recently-developed methods[2,3] for noncoherent combination of features extracted from coherent subaperture imaging, where subapertures are matched to scattering persistence angles.

Isolated, Dominant Scattering Centers: At high frequencies, radar backscattering from objects is well modeled as a sum responses from individual *scattering centers*.[1] Also, at sufficiently high resolutions, scattering centers on the object become resolved, and resolved scattering center responses have both stable phase responses and stable polarimetric response properties.[3,4] As a result, 3D location information inferred from scattering phase is sufficiently stable to permit 3D object reconstructions using interferometric SAR (IFSAR) techniques. At high resolutions, limited persistence of scattering is no longer dominated by scintillation effects, but instead relates to object shape. Furthermore, polarimetric features extracted from scattering centers are useful parameters to describe local geometry of the object.

3.1. Polarimetric, Wide-Angle IFSAR Processing for 3D Reconstruction

Based on the above considerations, we propose a wide-angle object reconstruction that employs IFSAR processing to arrive at 3D spatial scattering from processing of limited-angle apertures, along with noncoherent combinations of these points over wider angle apertures. We summarize the approach as follows. We collect data needed to form a pair of coherent SAR images at two closely-spaced elevation angles; the frequency and azimuth extent of this data-set pair are sufficiently large to obtain high-resolution images in which most scattering centers on the images are resolved. Standard tomographic image formation is used, so we implicitly assume that scattering amplitude is persistent and approximately constant across each of these limited-angle measurement apertures. From each pair of images, which we refer to as an IFSAR pair, we estimate the 3D location scattered energy corresponding to high-amplitude image pixels; the height of the scattering response, measured orthogonally to the image plane, is computed from the phase difference of corresponding pixels from the two images, using standard IFSAR processing methods.[5] Each 3D point is attributed with polarization features along with the center azimuth and elevation angle for measurements used to form this IFSAR image pair. This process is repeated for several IFSAR image pairs whose center angles span a wide range. Finally, the 3D points are noncoherently combined and rendered for visualization. The resulting data is of high dimension, and subsets of the data are rendered using color and transparency to visualize selected attributes.

IFSAR Processing: We process each IFSAR image pair as follows. We determine all image pixels whose radar cross section (RCS) is above a fixed threshold. If single-polarization imagery is available, the RCS is computed as the pixel magnitude; when two or more polarizations are measured, the RCS is computed as the

root-mean-square (RMS) sum of pixel magnitudes over the available polarizations. For each pixel exceeding the RCS threshold, we take its slant-plane downrange and crossrange location (x_s, y_s) as the pixel center, and compute its height from the slant plane using the difference in phase between the pixel value from the SAR image centered at $(\phi_k, \psi_k + \Delta\psi)$ and the image centered at (ϕ_k, ψ_k); that is,

$$z_s = \frac{\lambda}{4\pi\Delta\psi}\left[\angle s_2 - \angle s_1\right] \tag{2}$$

where λ is the radar wavelength at the center frequency, $\Delta\psi$ is the elevation difference angle of the IFSAR pair, and s_1 and s_2 are the pixel values from the two images. This 3D location is transformed from the local slant-plane coordinate system to a coordinate (x, y, z) in an absolute, target-centered coordinate system. We refer to this (x, y, z)-point as an "IFSAR point". We also test whether $|s_1| \approx |s_2|$ and reject points whose relative amplitudes are dissimilar, since amplitude dissimilarity indicates that the pixel values may not result from a single dominant scattering term, in which case the height estimate in (2) may be significantly biased.[6]

We associate with each IFSAR point several features: the center aspect (ϕ_k, ψ_k) of the IFSAR image pair, and the (possibly polarimetric) response amplitude. Thus, each IFSAR point is attributed with a feature vector of dimension 3–10 depending on the number of polarization channels measured.

Polarimetric Features: The response amplitude may be a single RCS value or a polarimetric characterization of amplitude. If full-polarization measurements are available, the amplitude is characterized by the 2×2 complex-valued matrix of scattering amplitudes from each of the four component polarizations. We form a Pauli-basis decomposition of this scattering matrix[7]

$$[S] = A\left[\cos(\alpha)[S]^t + e^{j\phi}\sin(\alpha)\left(\cos(\theta)[S]^d_0 + \sin(\theta)[S]^d_{45}\right)\right] \tag{3}$$

where $0^\circ \le \alpha \le 90^\circ$, $-45^\circ \le \theta \le 45^\circ$, and where the Surface-Dihedral-Tilted Dihedral basis is

$$[S]^t = \frac{1}{\sqrt{2}}\begin{bmatrix} 1 & 0 \\ 0 & 1 \end{bmatrix} \qquad [S]^d_0 = \frac{1}{\sqrt{2}}\begin{bmatrix} 1 & 0 \\ 0 & -1 \end{bmatrix} \qquad [S]^d_{45} = \frac{1}{\sqrt{2}}\begin{bmatrix} 0 & 1 \\ 1 & 0 \end{bmatrix}$$

The matrix $[S]^t$ represents an ideal trihedral (or other odd-bounce scattering object, such as a flat plate or a sphere), $[S]^d_0$ represents a horizontally-oriented dihedral (an even-bounce scattering term), and $[S]^d_{45}$ represents a diagonally-oriented dihedral (also even-bounce). Thus, the decomposition in equation (3) expresses the scattering matrix as a decomposition of these three canonical terms.

The real parameters A, α and θ, in particular, provide information about the physical characteristics of the dominant scattering mechanism in the resolution cell. The parameter α represents the mixture fraction of the trihedral and dihedral components; for $\alpha = 0$ the scattering center is entirely a trihedral component, and for $\alpha = 90^\circ$ it is entirely a dihedral. The angle θ gives the orientation angle of the dihedral term. A represents the overall RCS of the scattering center.

To summarize, IFSAR processing provides (x, y, z) locations of scattering centers that are persistent about a region centered at azimuth and elevation (ϕ_k, ψ_k). Scattering RCS A and polarimetric features such as α and θ further characterize the points. Thus, the radar signal processing output is a set of (x, y, z) locations, each attributed with several real-valued feature parameters.

4. VISUALIZATION TECHNIQUES

A set of three-dimensional points, each with the potential to have multiple real-valued features associated with it, needs to be visualized. One prevalent technique that could have been used would have been to take the point data and try to create surfaces from it. Given the nature of the data set, with its noise, these reconstruction techniques were deemed impracticable. Instead, two different, but complimentary, volume visualization techniques were applied to the data.

4.1. Volume Rendering

Volume Rendering is a technique whereby a three-dimensional scalar field is displayed without using any geometric primitives. The three-dimensional scalar field is comprised of volume pixels, or voxels. Each voxel can contain a scalar. In this case, the scalar could be the magnitude of the radar cross-section. Color and opacity are assigned to the scalar values of each voxel of the data set being visualized. By using a transfer function, each voxel sample can be shaded and projected onto a plane to form images.

Typically the volume rendering technique has been applied to extracting views of a surface or set of surfaces. In this case however, the data is not represented in terms of a voxel. Instead it is represented as point data that can have multiple scalars assigned to it. A rectilinear grid of size 1024^3 was created and the point data interpolated onto it. Each voxel could potentially contain a multiple number of points, each with its multiple scalar values. An algorithm selected the point data with the highest RCS value to reside within each voxel. An appropriate transfer function based on the RCS value was then applied. Lower RCS valued voxels had a lower amount of opacity. Higher RCS valued voxels had a higher amount of opacity. The Visualization Toolkit[8] (VTK), an open-source program from Kitware, was used to volume render the data. Due to the nature of the data, the image contained a pixilated look. In addition, we felt that it was inappropriate to apply a volume-based technique to point-based data. A second, point-based approach was then used.

4.2. Volume Cloud

A volume cloud technique is better suited to use with point data. With the volume rendering technique, point data is interpolated onto a rectilinear grid, and then the transfer function is applied to generate an image. With the volume cloud technique, the transfer function is applied directly to the points and rendered in a 3D conceptual package called Maya as a collection of points, or a cloud. Once again, opacity is applied to the points based on the RCS value. Singular points (or noise) are rendered but tend to disappear because of the size of the point and its transparency. Groups of points show up more readily. Color is applied using different transfer functions to highlight different scalar attributes.

5. BACKHOE RECONSTRUCTION EXAMPLES

In this section we present 3D representation and visualization results using the proposed sparse aperture reconstruction techniques applied to synthetic monostatic backscatter predictions of a backhoe.

5.1. Wide-Angle Backhoe Data

The data used in this study consists of scattering predictions of a backhoe shown in Figure 2.

Figure 2. Backhoe facet model used in Xpatch scattering predictions.

A facet model of the backhoe, along with the Xpatch scattering prediction program, is used to generate fully-polarimetric, monostatic backscattering predictions. For this study we consider a sparse sampling of the full data dome, as follows. XpatchT is used to generate SAR slant plane images with 2in×2in resolution. We synthesize SAR image pairs, where the kth image pair has center azimuth and elevation at (ϕ_k, ψ_k) and $(\phi_k, \psi_k + \Delta\psi)$ and where

$$\phi_k \in [0^\circ, 5^\circ, \ldots, 355^\circ]; \qquad \psi_k \in [0^\circ, 5^\circ, \ldots, 85^\circ]; \qquad \Delta\psi = 0.05^\circ \tag{4}$$

Each image thus requires backscattering measurements over a frequency band of approximately 8–12 GHz and an angle span of approximately 24° centered at its particular (ϕ_k, ψ_k) angle pair. For processing, we require that two images in each SAR image pairs be phase coherent with one another, but we do not require phase coherence from one IFSAR pair to another. This means, that separate radar platforms can measure SAR images with different (ϕ_k, ψ_k) center angles.

5.2. Backhoe 3D Reconstruction Results

We present four reconstruction examples that illustrate visualization techniques that use three different subsets of the scattering features described in Section 2.

Figure 3 shows three sample views of a 3D backhoe reconstruction. In this reconstruction, only the scattering RCS feature is shown. The RCS value is encoded by color, where red denotes highest RCS and green and blue denote successively smaller RCS values. In addition, RCS is also used to control voxel opacity. The reconstruction shows significant fine detail. The noncoherent combination of points provides a reconstruction that is filled from all angles, even though individual scattering terms may persist over much smaller angles, and is more reminiscent of optical imagery and traditional radar imagery. Multiple-bounce artifacts are seen below the front scoop and also to the sides of the rear scoop.

Figure 4 shows three sample views of the backhoe, where voxel opacity encodes RCS and color represents the center azimuth angle ϕ_k of the IFSAR image pair from which 3D point is extracted. The colors used to encode azimuth are best seen from the top view of the reconstruction. One can think of the center angle ϕ_k as the center angle around which the observed scattering center persists. If the scattering center is present for multiple views, then the response amplitudes at these views provides a sampling of the "antenna pattern" of that scattering center. Object substructures often have a common color, indicating that aspect angle may be useful as a feature for grouping scattering points into substructures. On the other hand, some substructures, especially rounded ones like the wheels and fenders, have multiple colors, indicating that only a fraction of the substructure is visible from any single limited-angle reconstruction of the object. A limited-angle reconstruction would show only a fraction of the object (e.g. the parts of the object in the figure with the same colors). This figure illustrates the benefit of wide-angle coverage of an object in the ability to reconstruct a 3D representation.

Figure 5 shows three sample views of the backhoe, where voxel opacity encodes RCS and color is used to depict a two-dimensional polarization state. In this image, the saturation of the color encodes the α parameter, and hue encodes the θ parameter. Colors closer to white or gray correspond to α near 0°, while fully-saturated colors correspond to α near 90°. The preponderance of gray in the figure indicates that most scattering centers have a strong trihedral component, and a relatively weak dihedral component.

Figure 6 shows three views in which opacity encodes RCS, colors are fully saturated, and the hue of the color encodes the polarization angle θ. One sees a strong correspondence between hue and local orientation angle of a scattering object, indicating that local orientation of many target substructures is encoded in the θ polarization angle.

These four examples show that target reconstructions rich in fine detail can be obtained from sparse, wide-angle reconstruction that are based on high-resolution IFSAR processing. Furthermore, scattering features such "antenna pattern" angles and polarization features provide geometrically-relevant information about local shape, and may be used to discriminate substructures on the target.

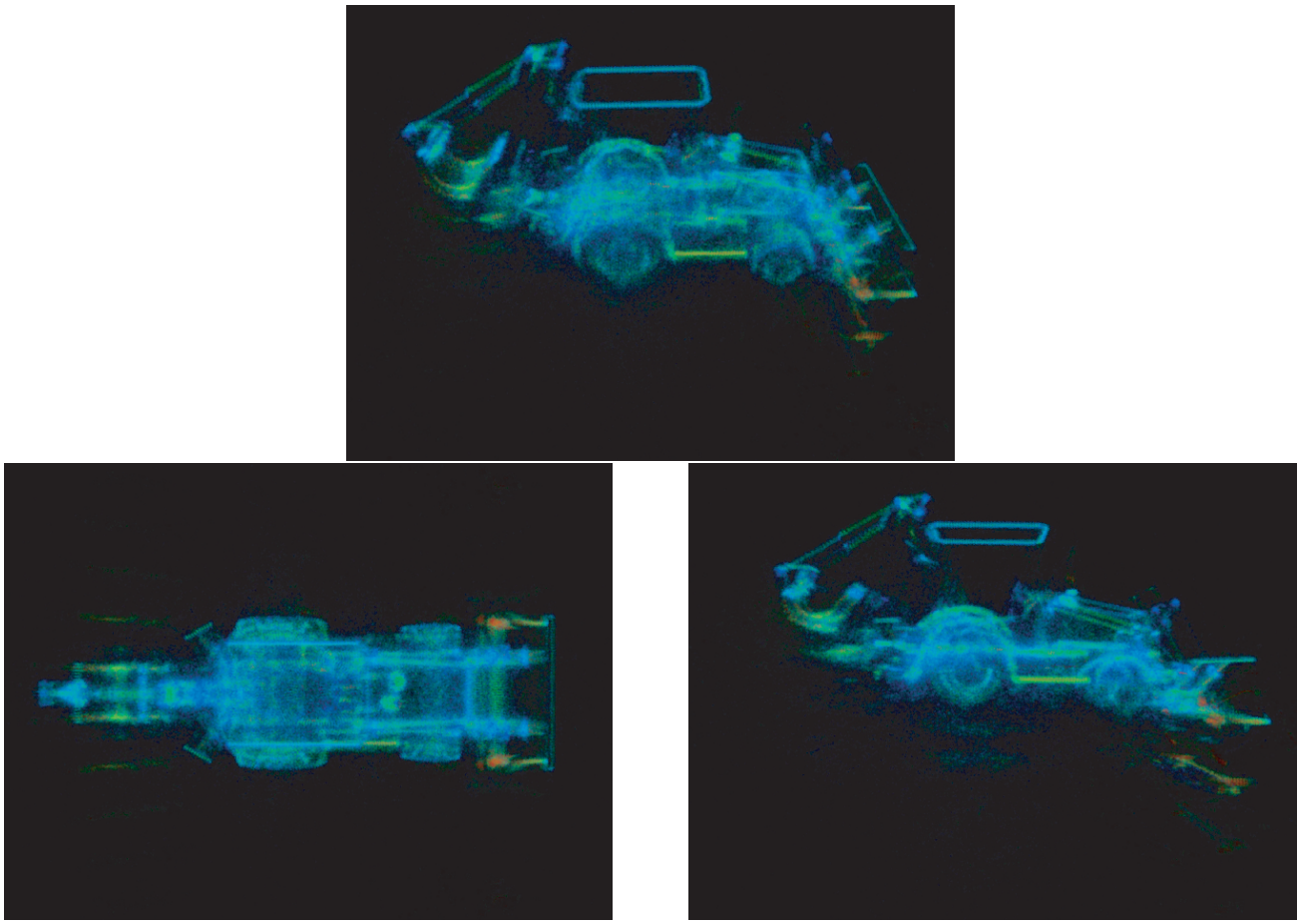

Figure 3. Volume cloud image of the backhoe with color representing the RCS magnitude.

6. CONCLUSIONS

We have presented a method for obtaining and visualizing 3D reconstructions of ground vehicles from high frequency, wide-angle monostatic radar backscattering measurements. Full reconstruction requires measurements over a dense grid in frequency-azimuth-elevation space, which imposes significant challenges for both data collection and data processing. The proposed method exploits properties of scattering physics to develop a reconstruction method that uses sparse aperture measurements; specifically, measurements are collected as a set of high-resolution interferometric SAR (IFSAR) image pairs that are distributed over wide angles. The IFSAR measurement samples are a sparse fraction of the full data dome measurements. Moreover, each image pair is processed coherently, but the results are combined noncoherently to form the 3D reconstructions. The noncoherent combination is significant, in that it relaxes the requirement for phase coherence across wide angle apertures; in particular, multiple radar measurement platforms operating incoherently from one another are able to collect data for this reconstruction.

The IFSAR processing results in a set of 3D spatial point locations of scattering centers, each attributed by several real-valued features. Analysis and visualization of this high-dimensional data represents a second challenge. We present rendering results in which volume clouds with colors and voxel opacity representing scattering features associated with the data. Results are presented in which scattering amplitude, polarization parameters, and observation angle parameters are represented in the reconstructions. The reconstructions indicate the power of the proposed visualization techniques for understanding high-dimensional point data, and provide a qualitative analysis and comparison tool for assessing the utility of these radar features for target recognition, structure extraction, and classification.

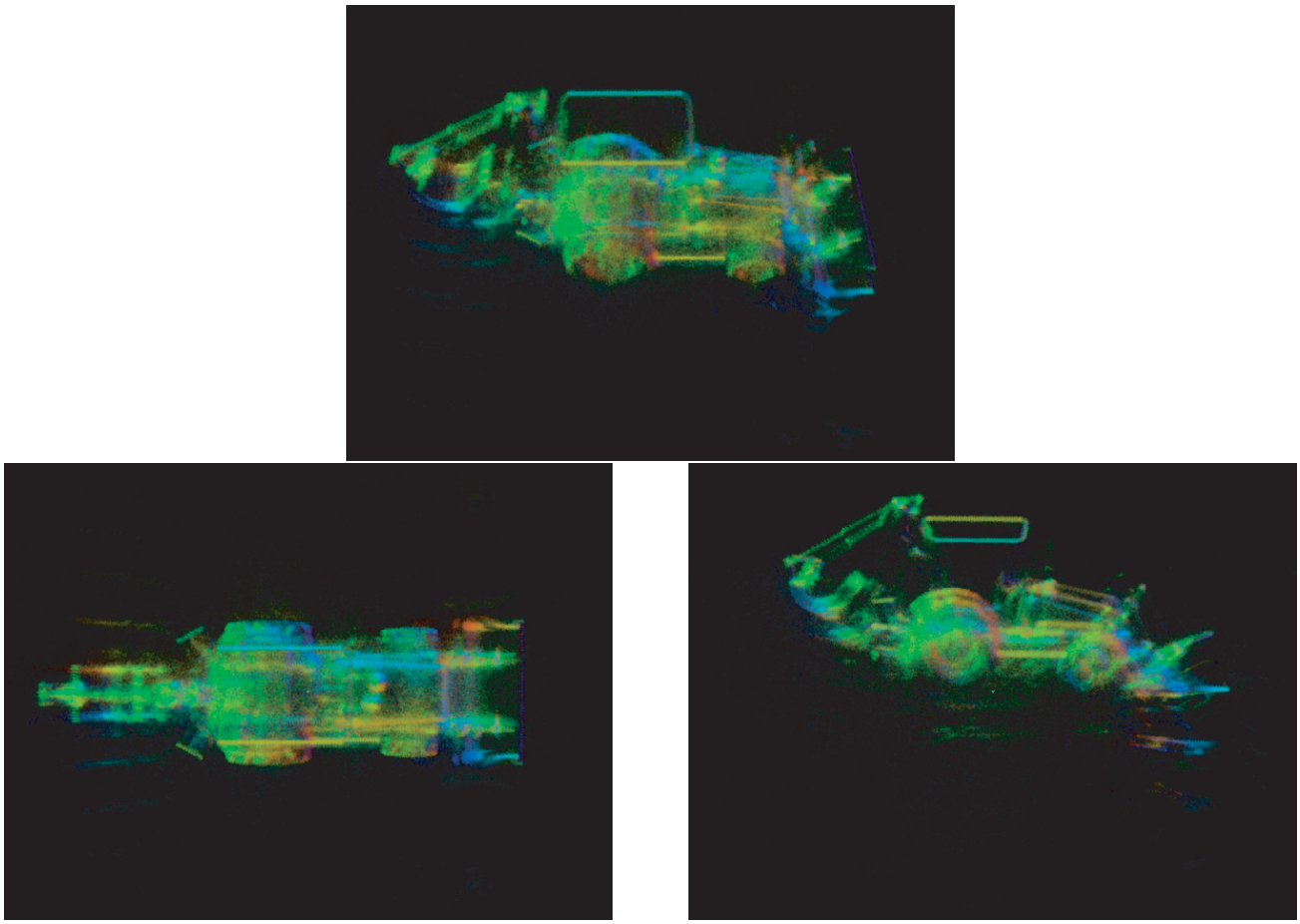

Figure 4. Volume cloud image of the backhoe with color representing the azimuth angle ϕ_k, associated with the scattering point.

REFERENCES

1. L. C. Potter and R. L. Moses, "Attributed scattering centers for SAR ATR," *IEEE Transactions on Image Processing* **6**, pp. 79–91, January 1997.
2. R. Moses, L. Potter, and M. Çetin, "Wide angle SAR imaging," in *Algorithms for Synthetic Aperture Radar Imagery XI (Proc. SPIE Vol. 5427)*, E. G. Zelnio, ed., April 2004.
3. R. Moses, E. Ertin, and C. Austin, "Synthetic aperture radar visualization," in *Proceedings of the 38th Asilomar Conference on Signals, Systems, and Computers*, (Pacific Grove, CA), November 7–10 2004.
4. Y. Akyildiz, "Feature extraction from synthetic aperture radar imagery," Master's thesis, The Ohio State University, August 2000.
5. C.V. Jakowatz, D.E. Wahl and P.H. Eichel, *Spotlight-Mode Synthetic Aperture Radar: A Signal Processing Approach*, Kluwer Academic Publishers, Boston, MA, 1996.
6. C. Austin and R. Moses, "IFSAR processing for 3D target reconstruction," in *Algorithms for Synthetic Aperture Radar Imagery XII (Proc. SPIE Vol. 5808)*, E. G. Zelnio, ed., March 2005.
7. E. Ertin and L. C. Potter, "Polarimetric classification of scattering centers," *IEEE Trans. on AES* , July 2000.
8. W. Schroeder, K. Martin, and B. Lorensen, *The Visualization Toolkit*, Kitware, Inc, 3rd ed., 2002.

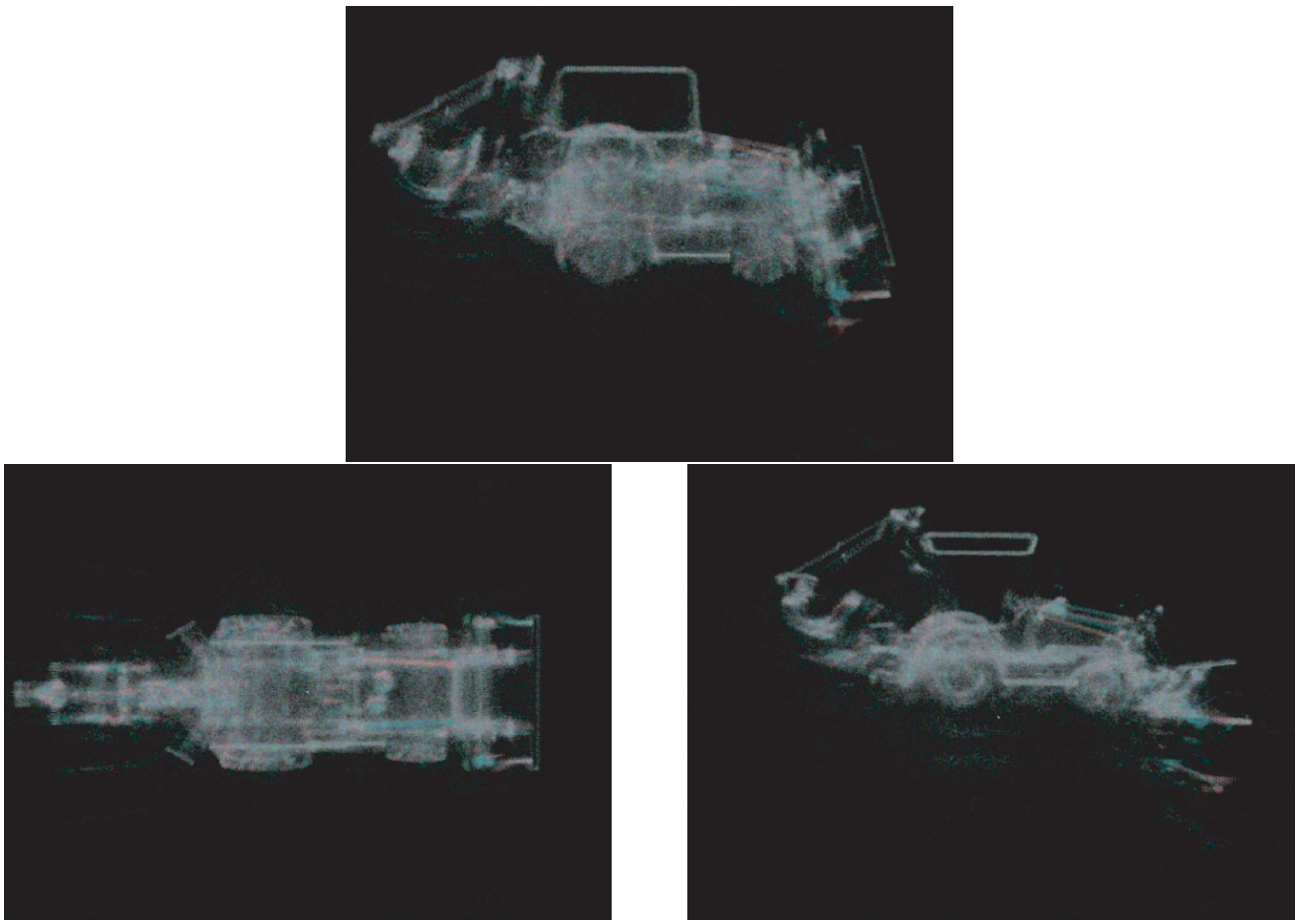

Figure 5. Volume cloud image of the backhoe with color representing the polarization parameters (α, θ), where color saturation encodes α and hue encodes θ. Gray values correspond to $\alpha \approx 0^\circ$ (scattering dominated by odd-bounce components), and fully-saturated colors correspond to $\alpha \approx 90^\circ$ (scattering dominated by dihedral components).

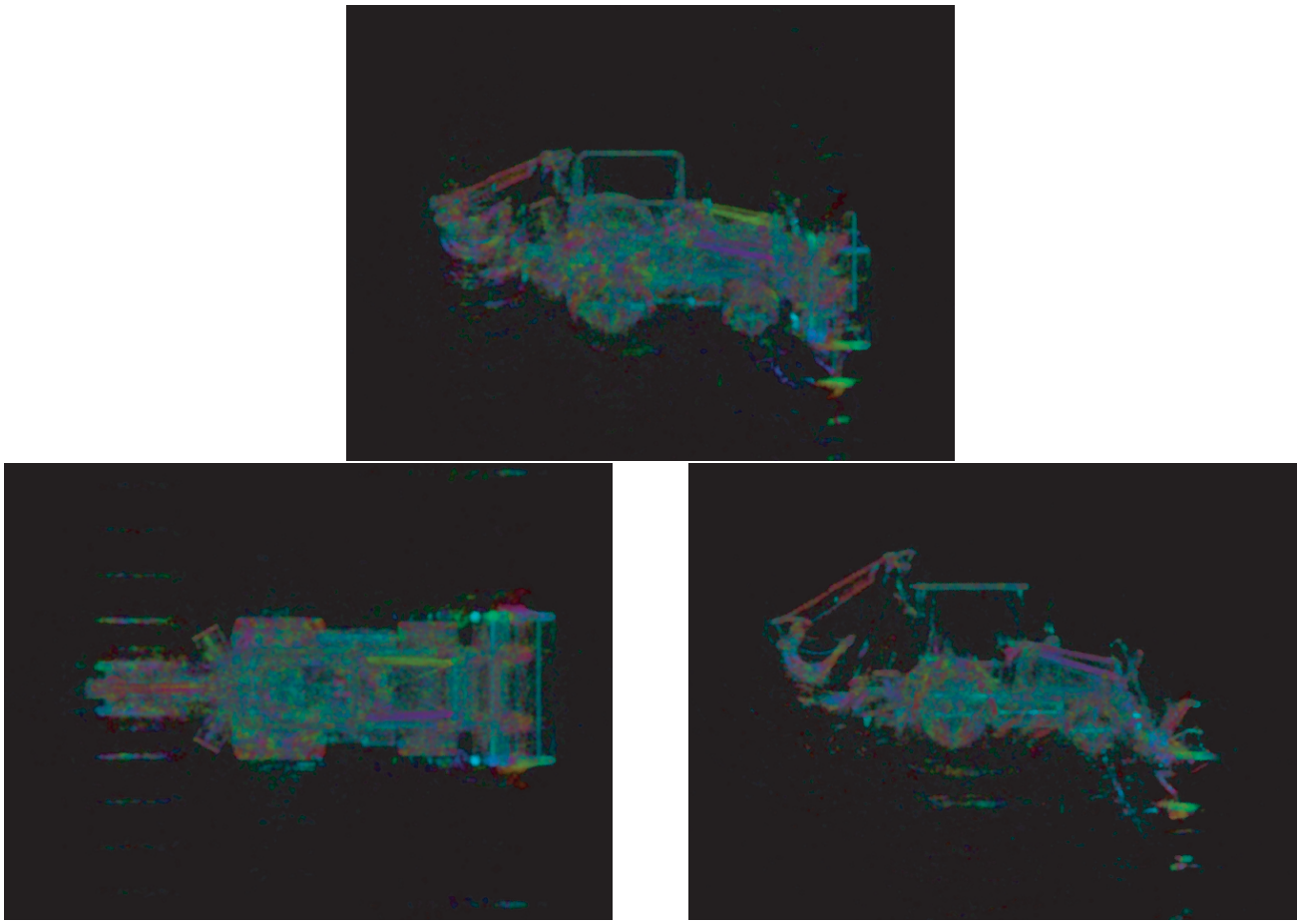

Figure 6. Volume cloud image of the backhoe with color representing the polarization parameter θ, where $\theta = -45^\circ$ is red, $\theta \approx 0^\circ$ is green, and $\theta = +45^\circ$ is blue.